

Regularities in pressure filtration of fine and colloidal suspensions

Sasanka Raha ^a, Kartic C. Khilar ^b, Prakash C. Kapur ^a, Pradip ^{a,*}

^a *Tata Research Development and Design Centre, 54B Hadapsar Industrial Estate, Pune-411013, India*

^b *Department of Chemical Engineering, Indian Institute of Technology, Mumbai-400076, India*

Abstract

A number of interesting and potentially useful regularities have been observed in high pressure batch filtration of fine and colloidal suspensions carried out to equilibrium under a wide variety of physical and chemical process conditions. Two such regularities are described here.

The first regular behavior, demonstrated by a large number of colloidal suspensions, can be represented by the Pareto profile, which relates filtration rate with solid content of filter cake at equilibrium. The profile is found to be a strong function of material fineness but is seemingly independent of physical and chemical process conditions. Since it can be treated as a constrained performance benchmark for the filtration of a suspension, it is germane for evaluating the filtration process in terms of two of its more important process measures, namely, kinetics and maximum extent of dewatering that is achievable. The Pareto regularity reflects the fact that in general it is not feasible to improve both measures simultaneously in a batch filtration which is driven to equilibrium, and any process modification may improve one measure but invariably at the expense of the other.

The second regular behavior, namely, self-similarity in pressure filtration is demonstrated for filtration of wide variety of varying materials and process conditions. Simple transformation and scaling of slurry filtration data with critical solid volume fraction and critical time at the transition from cake formation stage to cake consolidation stage translate the filtration curves into a form which are remarkably self-similar. This self-preserving behavior is demonstrated for a wide variety of experimental data under varying physical and chemical process conditions for different colloidal systems. Some implications of the regularities are discussed.

Keywords: Pressure filtration; Kinetics; Extent of dewatering; Pareto profile; Self similarity; Mathematical model; Particulate processing

1. Introduction

Over the years, pressure filtration has been studied experimentally and modeled theoretically by many investigators (Bai and Tien, 2005; Banda and Forssberg, 1988; Besra et al., 2002; Burger et al., 2001; Buscall and White, 1987; de Kretser et al., 2001; Glover et al., 2001,

2004; Holdich, 1993; Kapur et al., 2002; Landman et al., 1991,1995; Landman and White, 1997; Lu et al., 1998; Raha et al., 2005a,b, 2006; Ruth, 1946; Sis and Chander, 2000; Shirato et al., 1986; Stamatakis and Tien, 1991; Tien, 2002; Tao et al., 2003; Tiller and Yeh, 1987; Tiller and Kwon, 1998; Usher et al., 2001; Wakeman et al., 1991; Wu et al., 2003; Zhao et al., 2003a,b). It is known that pressure filtration generally comprises two stages involving cake formation and cake consolidation. The conventional filtration models (Ruth, 1946; Tiller and Yeh, 1987; Tiller and Kwon, 1998; Wakeman et al.,

Table 1
Powders used in the investigation

Powder		Mean particle size (μm)	Source (from Horiba particle size analyzer)
Alumina	A16 SG	0.34	Alcoa-ACC Industrial Chemical Ltd.
	A16	0.36	Alcoa
	SM8	0.29	Baikowsky
	CR6	0.35	
	CR1	1.09	
	Nano	0.25	Inframat Advanced Materials
Zirconia	E101	0.9	MEL Chemical
	Kaolin	1.12	Ward's Natural Establishment, Inc.
Iron oxide		0.51	Toda Kogyo Corp.

1991) mainly deal with the cake formation stage. The more rigorous and unified models for both cake formation and cake consolidation stages proposed recently (Burger et al., 2001; Buscall and White, 1987; Holdich, 1993; Landman et al., 1991, 1995; Landman and White, 1997; Raha et al., 2005a,b, 2006; Shirato et al., 1986; Stamatakis and Tien, 1991; Tien, 2002; Tiller and Yeh, 1987; Tiller and Kwon, 1998; Wakeman et al., 1991; Zhao et al., 2003a,b) are based on coupling of material independent equations of continuity and momentum with material specific constitutive properties, namely, compressibility and permeability (or hindered settling function, flux density function or specific cake resistance). Apart from the fact that implementation of model equations requires fairly involved numerical procedures (Burger et al., 2001; Landman et al., 1995), estimation of the constitutive properties in these comprehensive models, essential for carrying out

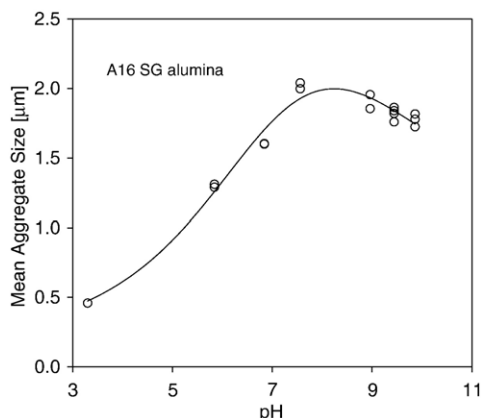


Fig. 1. Aggregate size as a function of pH for A16 SG alumina.

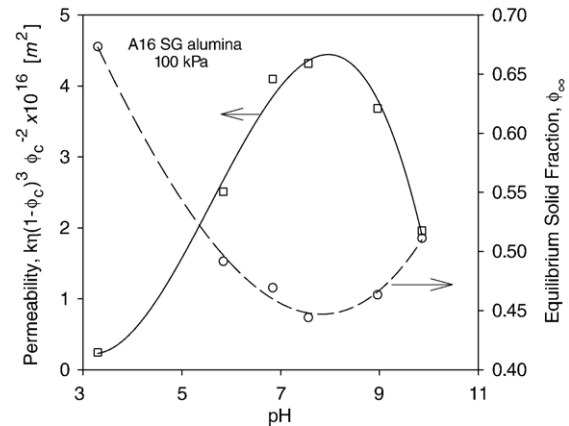


Fig. 2. Permeability and equilibrium solid fraction as a function of pH for A16 SG alumina.

simulation studies, is not exactly a trivial task (de Kretser et al., 2001; Tien, 2002).

Since filtration can vary a great deal depending upon the process conditions employed, it is of considerable importance to ascertain if process dynamics and overall dewatering performance under widely different conditions are subjected to any underlying regularities or patterns of relationship. Here we identify and discuss a couple of such behaviors in the pressure filtration processes: one, presence of a Pareto optimum for filtration kinetics and extent of dewatering and two, self-similarity of filtration curves.

2. Materials and methods

Standard fine powders (alumina, zirconia, kaolin and iron oxide) selected for the investigation and their

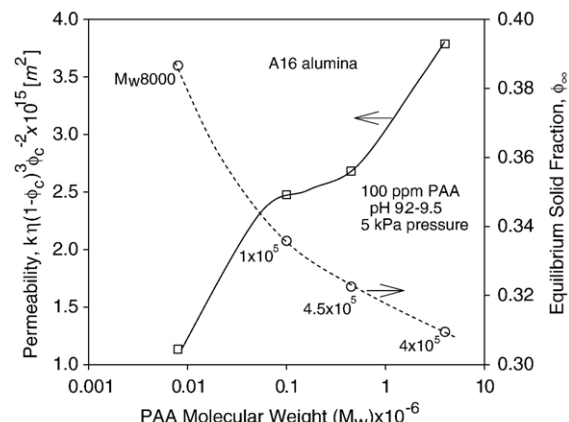


Fig. 3. Effect of PAA molecular weight on permeability and equilibrium solid volume fraction of the cake formed in batch filtration of A16 alumina.

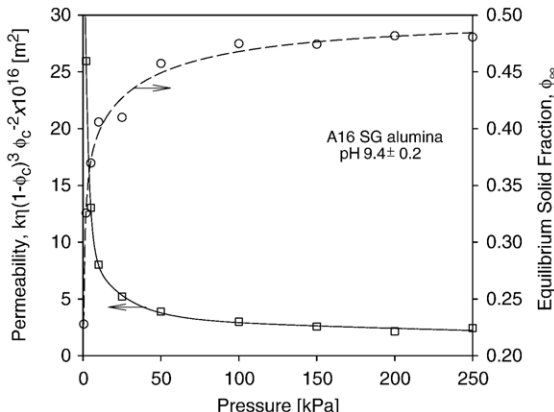


Fig. 4. Effect of applied pressure on permeability and equilibrium solid volume fraction of the cake formed in batch filtration of A16 SG alumina.

sources along with the corresponding mean particle size (d_{50}) as measured by Horiba particle size analyzer are listed in Table 1.

Particulate suspensions for pressure filtration tests were prepared using a standard procedure (Raha et al., 2005b, 2006). For preparation of slurry without additive, the suspension is dispersed on a magnetic stirrer for 2 min (except for some cases where 24 h conditioning is carried out). During this conditioning process pH adjustment is done using 4 N HNO_3 or NaOH . After conditioning, the suspension was ultrasonicated using a Branson 450 sonicator for 2 min using 50% duty cycle with 40 W power input.

Two different methods of additive addition were followed. In method A, the suspensions were prepared by adding powder to water containing polymer or surfactant of desired concentration on a magnetic stirrer. Magnetic stirring was done for 2 min. Following this, the suspensions were ultrasonicated using a Branson 450 sonicator for 2 min using 50% duty cycle with 40 W power input. In this method sonication was carried out after addition of additives. In method B, sonication was carried out before adding the additives. Following sonication, additive was added drop by drop with fast agitation on magnetic stirrer for 2 min followed by slow agitation for 3 min.

Pressure filtration experiments were carried out in a highly instrumented and programmable computer driven laboratory scale test rig, which has been described in detail elsewhere by its designers (de Kretser et al., 2001). Whatman filter paper No. 42 was used as the filter medium. Solid volume fraction is defined as the volume of solids represented as a fraction of total volume of suspension. The time vs. filtrate weight data is converted to time vs. solid volume fraction in the

chamber by material balance calculation. A large number of filtration tests were conducted to study the effect of various physical-chemical process parameters like pH, pressure, initial suspension height in filtration chamber, volume fraction of solids in feed, flocculant and surfactant types and their concentrations, different modes of polymer/surfactant addition and suspension preparation methods employed.

3. Mean-Phi model and estimation of parameters

A recently developed Mean-Phi (M-P) model for cake formation and cake consolidation in pressure filtration (Kapur et al., 2002; Raha et al., 2006) is employed here for analysis of the regularities. For sake of completeness, M-P model is described briefly in Appendix A.

The implementation of M-P model requires knowledge of three process parameters: k , which is common to stage 1 and stage 2, ϕ_c , which lies at the junction of these stages and ϕ_∞ , which determines the end of the process. These parameters were estimated by fitting stage 1 and stage 2 equations of M-P model (Eqs. (A3) and (A4)) to experimental data by minimizing a sum of the squares of errors in a nonlinear optimization scheme called SUMT.

4. Experimental results and discussion

4.1. Pareto profile

Filtration is a strong function of physical and chemical process variables such as applied pressure,

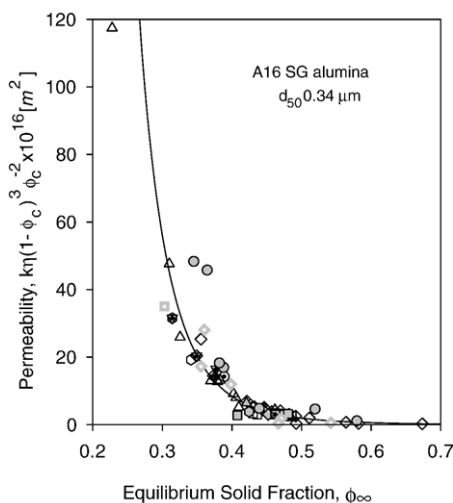


Fig. 5. Pareto profile benchmark for A16 SG alumina; refer to Table 2 for details of experimental conditions corresponding to each set of data (denoted by different symbols).

initial solid loading, slurry height, suspension pH, additive types and their dosage, slurry preparation method, etc. A number of studies (Banda and Forssberg, 1988; Besra et al., 2002; Bhattacharya and Vogelpohl, 1998; Glover et al., 2001, 2004; Mwaba, 1991; Watanabe et al., 1999; Wu et al., 2003) have shown that the manipulation of these process parameters usually leads to either faster rate of dewatering or lower cake moisture at equilibrium. As demonstrated in this investigation, there exists a regular Pareto profile benchmark which illustrates that it is not possible to simultaneously improve both kinetics and extent of dewatering at equilibrium in batch filtration of a material of given fineness.

Filtration characteristics strongly depend on particle-particle interaction and the state of aggregation of suspension. The state of aggregation of suspension, in turn, depends on the surface charge of particles. The point of zero charge (PZC) of A16 SG alumina, employed in present work, is pH 6.5 as measured by a standard electrophoresis technique using a Zetameter (Das et al.,

1997; Pradip et al., 1994; Ramakrishnan et al., 1996). As one moves away from PZC into acidic or basic pH range, surface charge on the particles increases leading to an increase in particle-particle repulsive force and enhanced dispersion of the suspension. Fig. 1 shows the size of A16 SG alumina aggregates measured by Horiba particle size analyzer as a function of the suspension pH. The suspension is, as expected, fully aggregated at or in close vicinity of PZC and becomes progressively more dispersed in increasing acidic or basic conditions. Along with changes in aggregate size, performance parameters of the filtration process are also significantly altered. Permeability of the filter cake plays a major role in dictating the time scale of filtration. It is shown in Appendix B that permeability of the growing cake in M-P model can be represented by the term $k\eta(1-\phi_c)^3\phi_c^{-2}$, where k is a lumped permeability factor in M-P model, η is fluid viscosity and ϕ_c is transition solid volume fraction at the junction of stage 1 and stage 2. The parameter ϕ_∞ , the volume fraction solids in the filter cake when

Table 2
Details of filtration tests using A16 SG alumina

Symbol	Conditioning	Additive	Amount (ppm)	Mol. wt.	Addition method	Pressure (kPa)	pH	ϕ_0	h_0 (m)
△	5 min	—	—	—	—	1, 2, 5, 10, 25, 50, 100, 200, 250	9.1–9.6	0.1	0.015, 0.02
□	5 min	—	—	—	—	100	9.2–9.7	0.03, 0.045, 0.06, 0.15 0.14, 0.17, 0.22, 0.3	
○	5 min	—	—	—	—	100	9.6–9.7	0.1	0.025, 0.035, 0.045
◇	5 min	—	—	—	—	100	3.3, 5.8, 6.8, 7.6, 9.0, 9.9	0.1	0.015
△	24 h	—	—	—	—	25, 50, 150, 200	8.8–9.0	0.1	0.02
△	24 h	—	—	—	—	100	8.9–9.1	0.1	0.01, 0.015, 0.02, 0.025, 0.03, 0.04
■	24 h	—	—	—	—	100	8.1–9.2	0.03, 0.04, 0.05, 0.075, 0.125, 0.15, 0.2	
○	5 min	PAA	100	8000	A	5	9.8	0.1	0.015
◆	5 min	PAA	100	30,000	A	5	9.8	0.1	0.015
▽	5 min	PAA	100	1×10^5	A	5	9.0	0.1	0.015
○	5 min	PAA	100	4.5×10^5	A	5	9.4	0.1	0.015
▽	5 min	PAA	100	4×10^6	A	5	9.4	0.1	0.015
▲	5 min	PAA	10	8000	A	5	9.7	0.1	0.015
▼	5 min	PAA	10	30,000	A	5	9.7	0.1	0.015
◆	5 min	PAA	10	1×10^5	A	5	9.7	0.1	0.015
○	5 min	PAA	10	4.5×10^5	A	5	9.6	0.1	0.015
○	5 min	PAA	10	4×10^6	A	5	9.7	0.1	0.015
■	5 min	Citric Acid	100	—	A	10	9.4	0.1	0.015
●	5 min	Na-Oleate	100	—	A	2	9.7	0.1	0.015
○	5 min	PAA	100	8000	B	5	4.4, 4.7, 5.2, 7.0, 9.2, 9.7	0.1	0.015
◆	5 min	PAA	100	4×10^6	B	5	2.1, 4.7, 5.6, 6.0, 7.0, 9.4	0.1	0.015

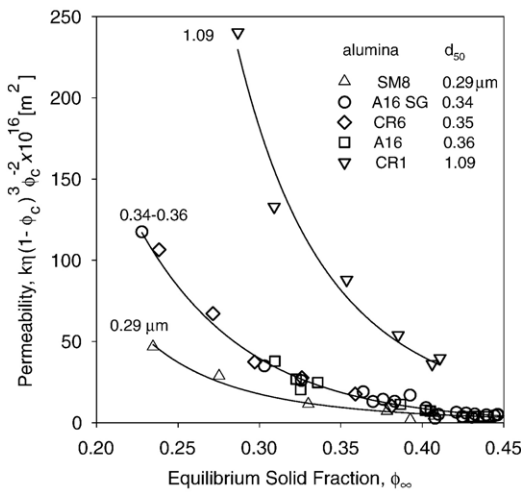


Fig. 6. Pareto profile benchmark for alumina powders of varying fineness.

equilibrium is reached, is a measure of the extent of compaction, that is, maximum dewatering possible under a set of process conditions.

The permeability parameter and equilibrium solid volume fraction (ϕ_{∞}) are plotted for A16 SG alumina as a function of pH in Fig. 2. A comparison with Fig. 1 shows that maximum aggregation, fastest filtration and least compaction (or dewatering) occur at about the same pH. The filtration rate increases steeply as pH is increased from 3.3 and then drops again from its highest value at about 7.5 as the suspension begins to redisperse with an increase in pH. It is reasonable to conclude that the agglomerates in the vicinity of PZC are relatively open and give rise to a more permeable bed, which result in faster kinetics. The behavior of equilibrium solid fraction with suspension pH tends to be opposite, exhibiting a minimum near PZC. In other words, the high permeability of filter cake around the point of zero charge is accompanied by high terminal moisture content of the filter cake and vice versa. Near PZC aggregated particles are heavier, larger and therefore exhibit faster filtration kinetics but entrap relatively more moisture at a given pressure. Higher surface charge (at pH's away from PZC) causes dispersion of particles leading to a considerable increase in the resistance to compact formation and slower filtration (Wakeman et al., 1991; Sis and Chander, 2000). The reduction in permeability of cake can also be attributed to the streaming potential effect observed for flows through extremely fine pores in packed bed of charged particles (Khilar, 1983). From Fig. 2 it is evident that with change in pH, the two performance measures namely the permeability parameter that controls the process time scale, and the

equilibrium solid fraction that represents the maximum dewatering possible, cannot be varied independently. It should be noted that the point of inflection on permeability and equilibrium solid fraction curves are observed at pH 8.0 in Fig. 2, the pH which is more than one pH unit away from the PZC of the powder (pH 6.5). The reason for this discrepancy is not understood at present. However it should be pointed out that similar deviations between PZC and maxima in shear yield stress have been reported earlier (Ramakrishnan et al., 1996).

Similar conclusions hold when polymers and surfactants are used to modify the aggregation. Fig. 3 shows the effect of 100 ppm poly acrylic acid (PAA) of different molecular weights on filtration of A16 alumina suspensions. With an increase in molecular weight, the permeability increases but invariably with a reduction in equilibrium solid fraction. This trend again illustrates the fact that the two performance measures, namely, the permeability parameter and the equilibrium solid fraction (or extent of dewatering) cannot be varied independently. Similar trends were obtained with addition of PAA of different chain length on a variety of powders. Apart from altering the suspension chemistry by polymer/surfactant addition and pH modification, trials were also conducted with physical process variables like filtration pressure, initial slurry height, initial solid volume fraction in feed slurry, etc. The effect of pressure on permeability and equilibrium solid fraction for A16 SG alumina is shown in Fig. 4. Again, equilibrium solid fraction increases and permeability decreases with an increase in pressure, and the two

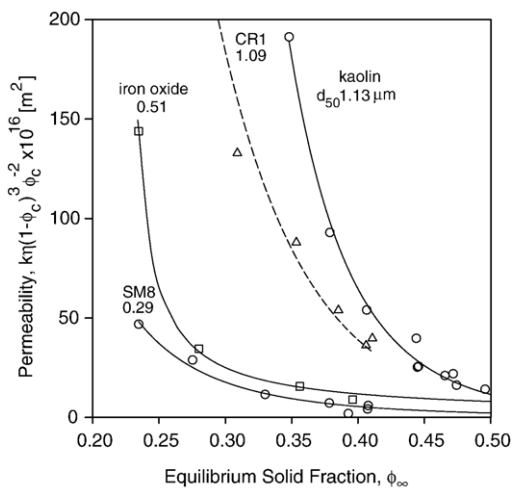


Fig. 7. Comparison of Pareto profile benchmark of different materials of varying fineness.

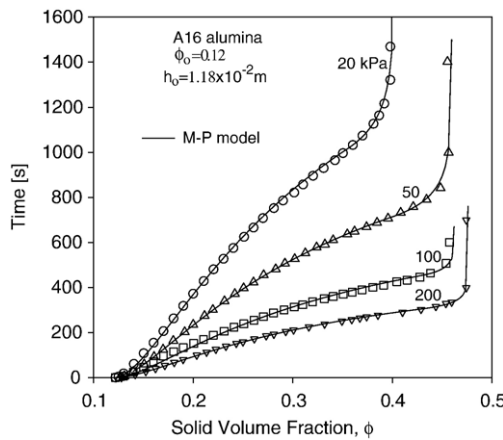


Fig. 8. Effect of pressure on filtration of A16 alumina under varying pressure conditions.

performance indices cannot be varied independently. It would seem that this is a fairly general phenomenon, which is encountered when chemical and physical process variables are varied in a systematic manner.

It turns out that the performance measures are interrelated by a regular Pareto profile for an exceptionally wide range of physical and chemical process conditions. This is illustrated in Fig. 5 where the permeability estimated by M-P model is plotted against equilibrium solid fraction for a large number of filtration tests on A16 SG alumina suspensions. The details of the process conditions are given in Table 2. The process conditions included: (1) 5 min short and 24 h long conditioning of suspension without addition of an additive, with systematic variations in pressure, initial solid content, feed slurry height in filtration chamber and pH, (2) addition of 100 ppm or 10 ppm PAA by method A where sonication is

carried out after addition of additives with systematic variations in molecular weight of the polymer, (3) addition of 100 ppm PAA of two molecular weights by method B where sonication is carried out before additive addition with systematic variations in pH, and (4) addition of 100 ppm citric acid and sodium oleate surfactants. It will be seen that all the data points collapse on a single curve independent of the suspension chemistry and other physical process variables, which is seemingly unique for a material of given fineness. Consequently, the performance measures cannot be varied independently, that is, any improvement in one index invariably leads to deterioration in the other index. This type of interrelationship belongs to the classical representation of the Pareto set such that each point on the Pareto curve in the figure represents a vector of optimum filtration measures, that is, strictly speaking, there are infinite numbers of optimal vectors and none is dominant over the rest. At an operational level, it is apparently not feasible to improve filtration kinetics without paying a penalty in equilibrium end moisture. As such, the regular Pareto profile can be exploited to benchmark the performance of a batch filtration process.

The regular Pareto behavior is also observed by alumina powders of different fineness, as illustrated in Fig. 6. The finest powder, SM8 alumina ($0.29\text{ }\mu\text{m}$ mean particle size) leads to the bottom most Pareto profile while the coarsest powder, CR1 alumina ($1.09\text{ }\mu\text{m}$ mean particle size) lies at the top. The Pareto profiles of intermediate size powders (A16 SG, CR6 and A16) lie between that of CR1 and SM8 alumina and appear to collapse because of close proximity of their fineness ($0.34\text{--}0.36\text{ }\mu\text{m}$). Evidently, the Pareto profile depends on the powder fineness and perhaps on its morphology.

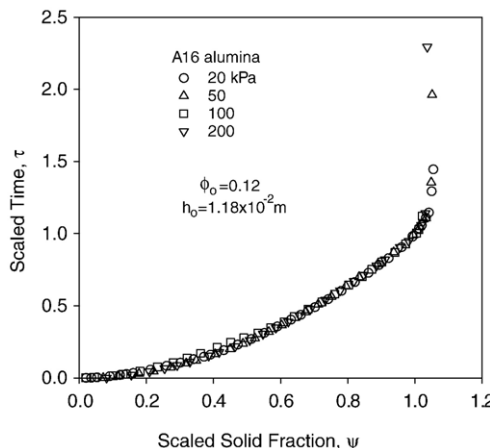


Fig. 9. Self-similarity for filtration of A16 alumina under varying pressure conditions.

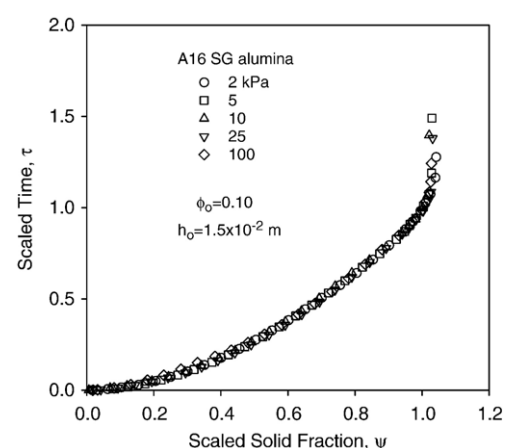


Fig. 10. Self-similarity for filtration of A16 SG alumina under varying pressure conditions.

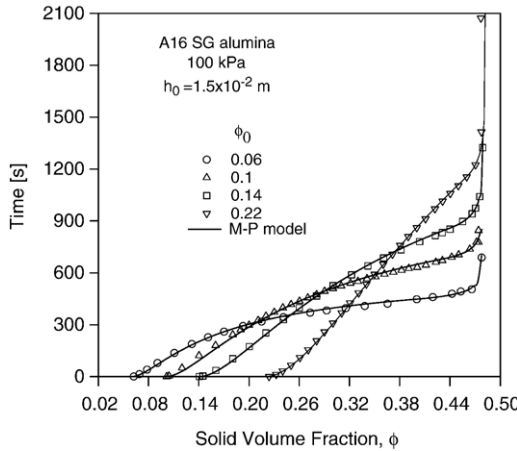


Fig. 11. Effect of initial solid volume fraction on filtration of A16 SG alumina.

The effect of particle size on filtration behaviour can be understood in terms of the increase in resistance to flow (decrease in permeability) with increasing fineness.

Fig. 7 compares Pareto profiles of kaolin and iron oxide with two alumina powders under a variety of process conditions. As size decreases in sequence from kaolin (1.13 μm), CR1 alumina (1.09 μm), iron oxide (0.51 μm) to SM8 alumina (0.29 μm), the associated Pareto profiles are pushed down, indicating lower permeability of finer powder cakes for same equilibrium solid fraction.

4.2. Self-similarity

In the previous section, we established a regular behavior in the performance of pressure filtration in terms of time scale and equilibrium solid content of the

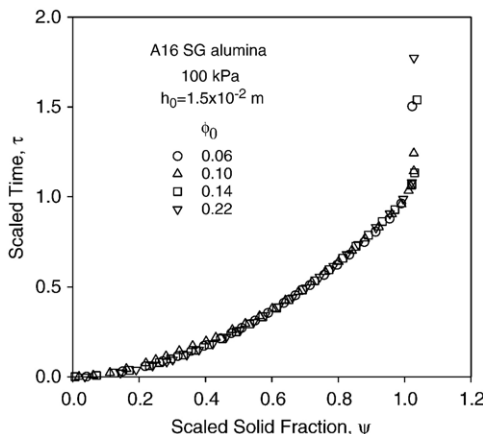


Fig. 12. Self-similarity for filtration of A16 SG alumina under varying ϕ_0 conditions.

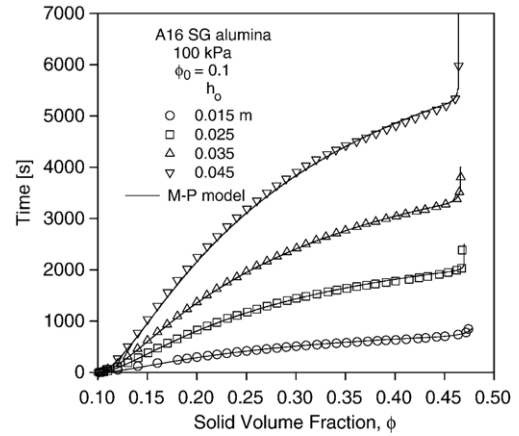


Fig. 13. Effect of initial slurry height on filtration of A16 SG alumina.

process. Here we discuss self-similarity in filtration of different materials with regard to filtration dynamics under widely varying process conditions for different materials. It is observed that the filtration curves of ϕ versus t become remarkably self-similar or self-preserving when these variables are rescaled with critical parameters ϕ_c and t_c , representing the cross over point of stage 1 into stage 2. The scaled parameters are defined as

$$\tau = \frac{t}{t_c} \quad (1)$$

and

$$\psi = \frac{\phi_c(\phi - \phi_0)}{\phi(\phi_c - \phi_0)} \quad (2)$$

The integrated form of cake formation equation (Eq. (A1) in Appendix A) is given by

$$t = \frac{h_0^2}{\beta_m^2} \left[1 - \frac{\phi_0}{\phi} \right]^2 \quad (3)$$

Dividing Eq. (3) by Eq. (A3) in Appendix A gives

$$\frac{t}{t_c} = \left[1 - \frac{\phi_0}{\phi} \right]^2 \left[1 - \frac{\phi_0}{\phi_c} \right]^{-2} \quad (4)$$

Rearranging Eq. (4) and substituting τ and ψ from Eqs. (1) and (2) yields the following modified form of stage 1 of M-P model

$$\tau = \psi^2 \quad (5)$$

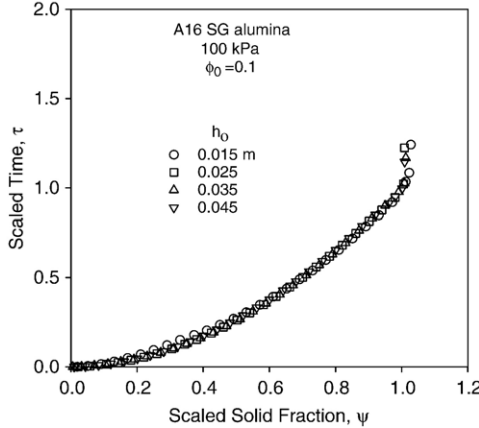


Fig. 14. Self-similarity for filtration of A16 SG alumina under varying h_0 conditions.

This implies that a plot of τ versus ψ under different process conditions should exhibit a self-similar behavior, at least in stage 1. Pressure is the one of the most commonly manipulated variables in filtration. The effect of pressure in the range of 20 kPa to 200 kPa on filtration of A16 alumina suspension at its natural pH is shown in Figs. 8 and 9 in terms of real and scaled variable, respectively. Fig. 8 demonstrates the close agreement between M-P model and experimental data in stage 1 as well as stage 2. All the curves in this figure collapse on a single curve in the transformed domain in Fig. 9, demonstrating the self-similar character of the pressure filtration curves. Interestingly, the self-preserving behavior holds in stage 2 also even though we are unable to derive it from the current form of M-P model. Fig. 10 shows similar results of a collapsed curve for filtration of a A16 SG alumina suspension under various

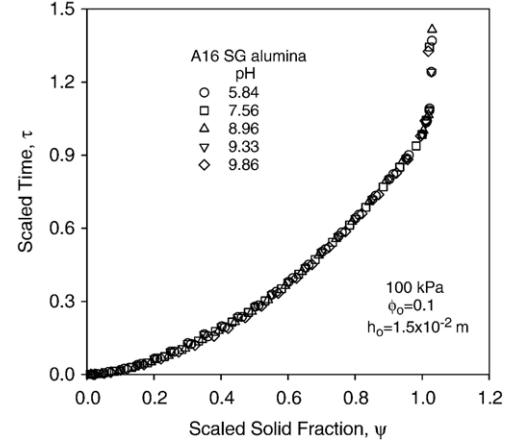


Fig. 16. Self-similarity for filtration of A16 SG alumina for varying pH conditions.

pressures. Fig. 11 shows the effect of initial solid volume fraction in the range of 0.06 to 0.22 on filtration of A16 SG alumina suspension under 100 kPa. Even though the filtration time increases with increasing initial solid content, the solid volume fraction in filter cake at equilibrium remains invariant, and the filtration curves are self-preserving in scaled variables as shown in Fig. 12. Similar results are obtained when initial slurry height in the filtration chamber is varied from 0.015 m to 0.045 m. The filtration data in Fig. 13 show that the end solid content of filter cake does not vary with initial slurry height. However, the filtration curves collapse on a similarity curve as demonstrated in Fig. 14.

The self-similar behavior is observed not only when physical process variables like pressure, initial solid

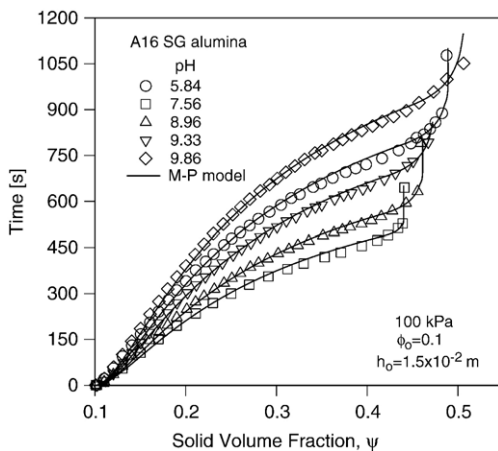


Fig. 15. Effect of pH on filtration of A16 SG alumina.

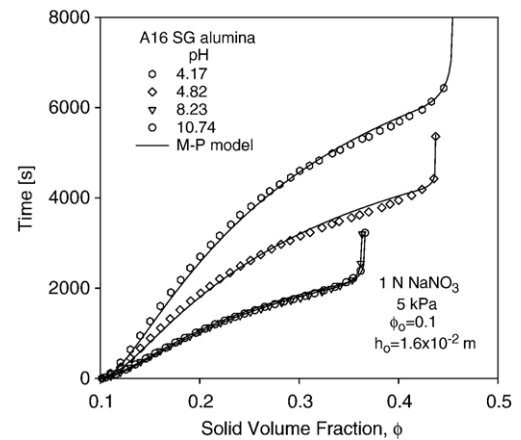


Fig. 17. Effect of pH on filtration of A16 SG alumina under high salt concentration.

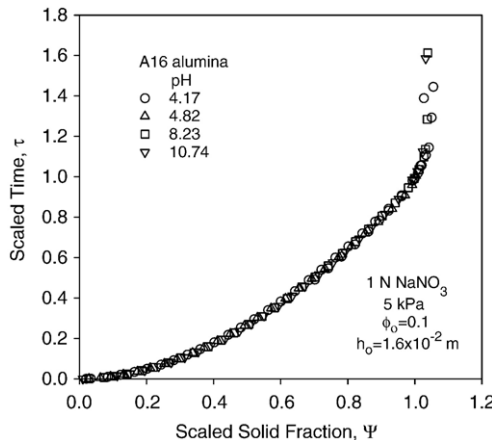


Fig. 18. Self-similarity for filtration of A16 SG alumina for varying pH conditions under high salt concentration.

volume fraction and initial slurry height are varied, but also for changes in chemical process conditions like suspension pH and additives. Fig. 15 for filtration of A16 SG alumina suspensions under 100 kPa pressure shows that the filtration rate increases rapidly in the pH range of 5.84 to 7.56, passes through a maximum and then decreases in pH range of 7.56 to 9.86. This variation is accompanied by an opposite trend in ϕ_∞ , namely, a decrease followed by an increase. That the filtration curves of this relatively complex behavior are also self-similar is well illustrated in Fig. 16.

Fig. 17 shows filtration of A16 SG alumina under different pH conditions in presence of high salt concentration (1 N NaNO₃). It is observed that increasing pH leads to coagulation, resulting in fast filtration and low final solid volume fraction even at pH 10.74. Again, the filtration curves at different pH in

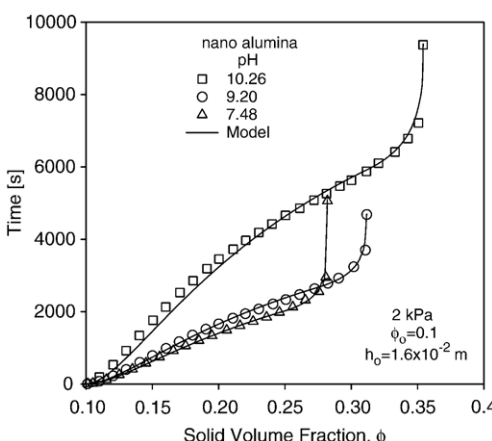


Fig. 19. Effect of pH on filtration of nano alumina.

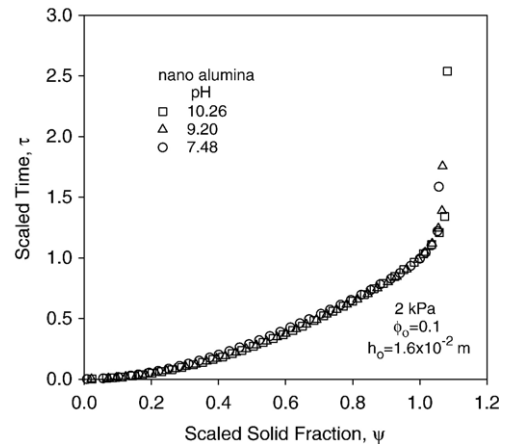


Fig. 20. Self-similarity for filtration of nano alumina under varying pH conditions.

presence of high salt concentration collapse in the scaled domain as shown in Fig. 18.

The filtration curves of nano alumina suspensions in Fig. 19 under different pH conditions indicate that the filtration behavior was qualitatively similar to that of coarser alumina powders. In this case also the fastest dewatering rate, at pH 7.48, is accompanied by lowest end solid content of filter cake, and the curves are self-similar in the transformed domain as shown in Fig. 20. The self-similar behavior is maintained in Figs. 21 and 22 when slurry modifiers or surfactants are added. Even powder mixtures, such as A16 SG alumina and E101 zirconia in 1:1 volume proportion, also give rise to self-preserving curves as seen in Fig. 23. Different materials under varying pressure and pH conditions are also self similar as shown in Fig. 24. In fact, very extensive

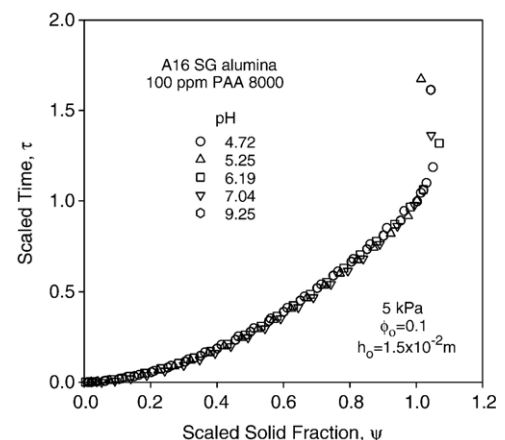


Fig. 21. Self-similarity for filtration of A16 SG in presence of 100 ppm of 8000 M_w poly acrylic acid under varying pH conditions.

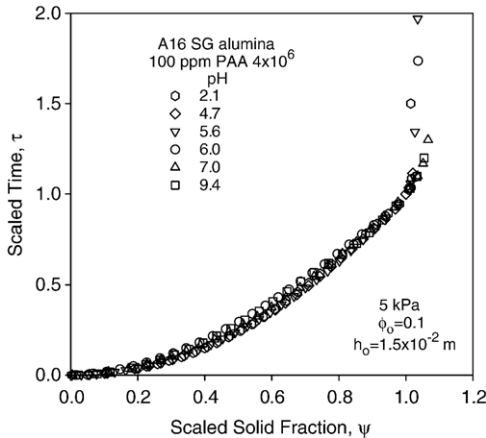


Fig. 22. Self-similarity for filtration of A16 SG in presence of 100 ppm of 4×10^6 M_w poly acrylic acid under varying pH conditions.

pressure filtration data for different alumina, zirconia and kaolin materials acquired under wide range of process conditions invariably exhibits the self-similar behavior.

5. Concluding remarks

Two regularities involving filtration overall performance and filtration dynamics are identified. These regularities, namely, 'Pareto profile' and 'self-similarity' are demonstrated for a wide variety of process conditions and suspensions of different materials. The 'kinetics-extent of dewatering Pareto profile' for a given material is independent of all process variables but a strong function of particle fineness. The Pareto profile benchmark signifies that it may not be possible to

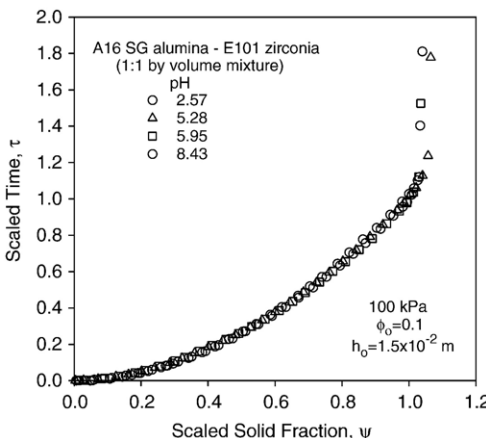


Fig. 23. Self-similarity for filtration of alumina-zirconia mixture under varying pH conditions.

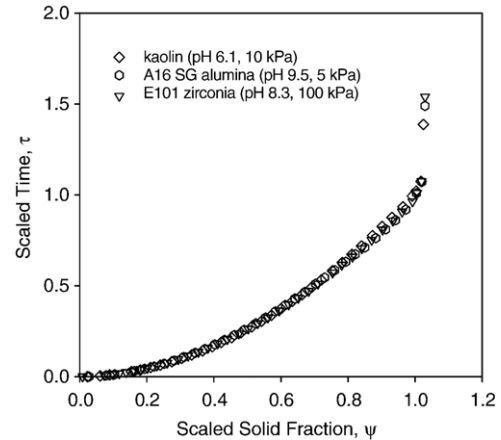


Fig. 24. Self-similarity for filtration of different materials under diverse conditions.

improve both kinetics and extent of dewatering simultaneously for batch pressure filtration driven to equilibrium by modifications of the process parameters and suspension chemistry. The Pareto regularity represents a constrained performance benchmark of the material being filtered and could be useful for evaluating the performance of the process.

The self-similar behavior in process dynamics is manifested by a straightforward transformation and scaling of slurry filtration data by critical solid volume fraction (ϕ_c) and critical time (t_c). Even though self-preserving behavior is observed over the full range of the filtration curve, at present the transformation can be derived from M-P model for stage 1 of filtration only. Its theoretical basis for stage 2 remain an unsolved problem. A wide variety of experimental data for batch pressure filtration under varying physical and chemical process conditions for different materials is demonstrably self-similar. The collapsed curve is a finger print of the material-filter system and it could have considerable utility for simulation and comparative evaluation.

Nomenclature

h_c	Filter cake height at any instant, m
h_s	Suspension layer thickness on top of cake, m
h_0	Initial suspension height, m
k	Lumped permeability factor including particle size, tortuosity and fluid viscosity
K_d	Darcy's permeability, m^2
K_{M-P}	Permeability estimated from M-P model, m^2
K_m	Lumped filtration resistance parameter of mean phi model defined in Eq. (A5)
L	Length of bed, m
m	Mass of dry cake per unit area, $kg\ m^{-2}$

R_m	Medium resistance, m^{-1}
R_t	Total resistance, m^{-1}
t	Time, s
t_c	Critical filtration time, s
V	Cumulative specific filtrate volume per unit area at filtration time t , m
V_z^f	Fluid superficial velocity, m s^{-1}

Greek letters

α	Specific cake resistance, m kg^{-1}
α_{M-P}	Specific cake resistance estimated from M-P model, m kg^{-1}
β_m	β defined in Eq. (A1), $\text{m/s}^{0.5}$
ΔP	Applied pressure, kPa
ϕ	Average volume fraction of solids in filtration chamber
ϕ_c	Critical average volume fraction of solids
ϕ_∞	Maximum solid content of cake at an applied pressure
ϕ_0	Initial volume fraction of solids
$\bar{\phi}$	Average volume fraction of solids in cake
η	Viscosity, Pa s
ρ_s	Solid density, kg m^{-3}
τ	Scaled time
ψ	Scaled solid volume fraction

Acknowledgement

Financial support for this work from Department of Science and Technology (DST), Government of India is gratefully acknowledged. We are grateful to Prof. Mathai Joseph, Executive Director, Tata Research Development and Design Centre for encouragement and support.

Appendix A. Mean Phi (M-P) model of pressure filtration

M-P model exploits a time-invariant uniform volume fraction of solids approximation for growing filter cake during cake formation and a time-dependent uniform volume fraction of solids approximation for cake consolidation.

The equation for cake formation is

$$\frac{dt}{d\phi} = \frac{2h_0^2\phi_0}{\beta_m^2\phi^2} \left(1 - \frac{\phi_0}{\phi}\right) d\phi \quad (\text{A1})$$

where t is filtration time, h_0 is initial slurry height, ϕ_0 and ϕ represent initial and average solid volume fraction in the chamber respectively.

The rate parameter β_m^2 is given by

$$\beta_m^2 = 2k \frac{(\phi_c - \phi_0)(1 - \phi_c)}{\phi_0 \phi_c^2} \Delta P \quad (\text{A2})$$

where k is a lumped permeability factor that includes particle size, tortuosity and fluid viscosity, ϕ_c is time-invariant uniform volume fraction solids in the cake at which transition from cake formation to cake consolidation takes place at filtration time t_c and ΔP is applied pressure.

The time for cake formation is represented as

$$t_c = \frac{h_0^2}{\beta_m^2} \left[1 - \frac{\phi_0}{\phi_c}\right]^2 \quad (\text{A3})$$

Model equation for consolidation stage is given by

$$\frac{dt}{d\phi} = K_m \frac{d\phi}{\phi(\phi_\infty - \phi)(1 - \phi)^3}; \quad \phi_c < \phi < \phi_\infty \quad (\text{A4})$$

with initial condition, $\phi = \phi_c$ at $t = t_c$ and ϕ_∞ is equilibrium solid volume fraction when filtration ceases. The lumped scalar K_m of the process time is given by

$$K_m = \frac{(h_0\phi_0)^2(\phi_\infty - \phi_c)}{k\Delta P} \quad (\text{A5})$$

Appendix B. Permeability in M-P model

Darcy's law is given as

$$V_z^f = \frac{K_d \Delta P}{\eta L} \quad (\text{B1})$$

where V_z^f represents fluid superficial velocity, K_d represents Darcy's permeability, η is fluid viscosity and L is the length of bed. The Darcy's law in Eq. (B1) is rewritten as

$$V_z^f = \frac{1}{\eta} \frac{\Delta P}{R_t} \quad (\text{B2})$$

where R_t is the total resistance.

Realizing that the resistance has two components, namely cake resistance and medium resistance, Eq. (B2) is rewritten as

$$\frac{dV}{dt} = \frac{\Delta P}{(\alpha m + R_m)\eta} \quad (\text{B3})$$

where, V is cumulative filtrate volume per unit area at

time t , α is the specific cake resistance, m is mass of dry cake per unit area and R_m is medium resistance.

Consider a situation where h_0 is the initial height of suspension with solid volume fraction ϕ_0 , h_c is height of cake at any instant with solid volume fraction ϕ^- and h_s is height of suspension above the formed cake with solid volume fraction ϕ_0 during cake formation process. Following mass balance across the cake one obtains

$$h_c + h_s = h_0 - V \quad (B4)$$

$$\bar{\phi} h_c + \phi_0 h_s = h_0 \phi_0 \quad (B5)$$

Combining Eqs. (B4) and (B5) results in

$$h_c = \frac{\phi_0 V}{\bar{\phi} - \phi_0} \quad (B6)$$

Using (B6) one can write

$$m = \bar{\phi} h_c \rho_s = \frac{\bar{\phi} \phi_0 \rho_s V}{\bar{\phi} - \phi_0} \quad (B7)$$

where ρ_s is solid density.

Clearly m is a function of $\bar{\phi}$ as well, in addition to ϕ_0 , ρ_s and V . After substituting Eq. (B7) into Eq. (B3) for m and integrating for constant $\bar{\phi}$ gives

$$\frac{t}{V} = \frac{\alpha_{M-P} \phi_0 \bar{\phi} \rho_s \eta}{2(\bar{\phi} - \phi_0) \Delta P} V + \frac{\eta R_m}{\Delta P} \quad (B8)$$

where α_{M-P} is specific cake resistance estimated using Eq. (B8).

From Eqs. (B1) and (B2), cake resistance for cake thickness $L = h_c$ (neglecting medium resistance) is given as

$$R_t = \frac{h_c}{K_d} \quad (B9)$$

Representing R_t in terms of specific cake resistance one gets

$$R_t = \alpha_{M-P} m = \alpha_{M-P} h_c \bar{\phi} \rho_s \quad (B10)$$

Comparing (B9) and (B10) correlates Darcy's permeability to specific cake resistance as

$$K_d = \frac{1}{\alpha_{M-P} \bar{\phi} \rho_s} \quad (B11)$$

In M-P model, the solid volume fraction of growing cake, $\bar{\phi}$, comes out of parameter tuning process, that is

used in Eqs. (B8) and (B11) for estimation of α_{M-P} and K_d . Henceforth we will define K_d estimated using $\bar{\phi}$ information of the M-P model as K_{M-P} , i.e. M-P model permeability. In M-P model development, $\bar{\phi}$ during cake formation is same as ϕ_c . Consequently, Eq. (B11) may be written as

$$K_{M-P} = \frac{1}{\alpha_{M-P} \phi_c \rho_s} \quad (B12)$$

Classical parabolic filtration rate equation is given as

$$V = \beta_m \sqrt{t} \quad (B13)$$

Comparison of Eq. (B8) with Eq. (B13) for negligible medium resistance and substituting $\bar{\phi}$ with ϕ_c leads to

$$\beta_m^2 = \frac{2(\phi_c - \phi_0) \Delta P}{\alpha_{M-P} \phi_0 \phi_c \rho_s \eta} \quad (B14)$$

Comparing Eq. (A2) of M-P model with (B14) yields

$$\alpha_{M-P} = \frac{\phi_c}{k \rho_s \eta (1 - \phi_c)^3} \quad (B15)$$

Substituting Eq. (B15) in (B12) we get

$$K_{M-P} = \frac{k \eta (1 - \phi_c)^3}{\phi_c^2} \quad (B16)$$

References

- Bai, R., Tien, C., 2005. Further work on cake filtration analysis. *Chem. Eng. Sci.* 60, 301–313.
- Banda, S.M.H., Forssberg, K.S.E., 1988. Structure variation in filter cakes from flocculated slurries. *Scand. J. Metal.* 17, 57–60.
- Besra, L., Sengupta, D.K., Roy, S.K., Ay, P., 2002. Flocculation and dewatering of kaolin suspensions in the presence of polyacrylamide and surfactants. *Int. J. Miner. Process.* 66, 203–232.
- Bhattacharya, I.N., Vogelpohl, A., 1998. Study on dewaterability of Lateritic nickel ore suspension using capillary suction time (CST) and settling tests. *Indian Chem. Eng. Section A* 40, 329–335.
- Burger, R., Concha, F., Karlsen, K.H., 2001. Phenomenological model of filtration processes: 1. Cake formation and expression. *Chem. Eng. Sci.* 56, 4537–4553.
- Buscall, R., White, L.R., 1987. The consolidation of concentrated suspensions: Part 1. The theory of sedimentation. *J. Chem. Soc., Faraday Trans.* 83, 873–891.
- Das, K.K., Pradip, Natarajan, K.A., 1997. The effect of constituent metal ions on the electrokinetics of chalcopyrite. *J. Colloid Interface Sci.* 196, 1–11.
- de Kretser, R.G., Usher, S.P., Scales, P.J., Boger, D.V., 2001. Rapid filtration measurement of dewatering design and optimization parameters. *AIChE J.* 47, 1758–1769.

Glover, S.M., Yan, Y.D., Jameson, G.J., Biggs, S., 2001. Polymer molecular weight and mixing effects on floc compressibility and filterability in 6th World Congress of Chemical Engineering. Melbourne, Australia.

Glover, S.M., Yan, Y.D., Jameson, G.J., Biggs, S., 2004. Dewatering properties of dual-polymer-flocculated systems. *Int. J. Miner. Process.* 73, 145–160.

Holdich, R.G., 1993. Prediction of solid concentration and height in a compressible filter cake. *Int. J. Miner. Process.* 39, 157–171.

Kapur, P.C., Raha, S., Usher, S., de Kretser, R.G., Scales, P.J., 2002. Modeling of the consolidation stage in pressure filtration of compressible cakes. *J. Colloid Interface Sci.* 256, 216–222.

Khilar, K.C., 1983. Effect of streaming potential on the permeability of sandstones. *I&EC Fundamentals* 22, 264–266.

Landman, K.A., White, L.R., 1997. Predicting filtration time and maximizing throughput in a pressure filter. *AIChE J.* 43, 3147–3160.

Landman, K.A., Sirakoff, C., White, L.R., 1991. Dewatering of flocculated suspensions by pressure filtration. *Phys. Fluids, A Fluid Dyn.* 3, 1495–1509.

Landman, K.A., White, L.R., Eberl, M., 1995. Pressure filtration of flocculated suspensions. *AIChE J.* 41, 1687–1700.

Lu, W.M., Huang, Y.P., Hwang, K.J., 1998. Methods to determine the relationship between cake properties and solid compressive pressure. *Sep. Purif. Technol.* 13, 9–23.

Mwaba, C.C., 1991. Surfactant-enhanced dewatering of graphite and hematite suspensions. *Min. Eng.* 4, 49–62.

Pradip, Premachandran, R.S., Malghan, S.G., 1994. Electrokinetic behaviour and dispersion characteristics of ceramic powders with cationic and anionic polyelectrolytes. *Bull. Mater. Sci.* 17, 911–920.

Raha, S., Khilar, K.C., Pradip, Kapur, P.C., 2005a. Rapid determination of compressive yield stress of dense suspensions by a mean-phi ($\bar{\phi}$) model of high pressure filtration. *Powder Technol.* 155, 42–51.

Raha, S., Khilar, K.C., Pradip, Kapur, P.C., 2005b. A Pareto profile benchmark for kinetics of filtration and extent of dewatering of fine and colloidal suspensions. *Ind. Eng. Chem. Res.* 44, 9364–9368.

Raha, S., Khilar, K.C., Pradip, Kapur, P.C., 2006. A Mean Phi model for pressure filtration of fine and colloidal suspensions. *Can. J. Chem. Eng.* 84, 83–93.

Ramakrishnan, V., Pradip, Malghan, S.G., 1996. Yield stress of alumina–zirconia suspensions. *J. Am. Ceram. Soc.* 79, 2567–2576.

Ruth, B.F., 1946. Correlating filtration theory with industrial practice. *Ind. Eng. Chem.* 38, 564–571.

Shirato, M., Murase, T., Iwata, M., 1986. Deliquoring by expression theory and practice. In: Wakeman, R.J. (Ed.), *Progress in Filtration and Separation*, vol. 4. Elsevier, Amsterdam.

Sis, H., Chander, S., 2000. Pressure filtration of dispersed and flocculated alumina slurries. *Miner. Metall. Process.* 17, 41–48.

Stamatakis, K., Tien, C., 1991. Cake formation and growth in cake filtration. *Chem. Eng. Sci.* 46, 1917–1933.

Tao, D., Parekh, B.K., Liu, J.T., Chen, S., 2003. An investigation on dewatering kinetics of ultra fine coal. *Int. J. Miner. Process.* 70, 235.

Tien, C., 2002. Comments on phenomenological model of filtration process: I. Cake formation and expression. *Chem. Eng. Sci.* 57, 2119–2120.

Tiller, F.M., Kwon, J.H., 1998. Role of porosity in filtration: XIII. Behavior of highly compactable cakes. *AIChE J.* 44, 2159–2167.

Tiller, F.M., Yeh, C.S., 1987. The role of porosity in filtration: Part XI. Filtration followed by expression. *AIChE J.* 33, 1241–1255.

Usher, S.P., de Kretser, R.G., Scales, P.J., 2001. Validation of a new filtration technique for dewaterability characterization. *AIChE J.* 47, 1561–1570.

Wakeman, R.J., Sabri, M.N., Tarleton, E.S., 1991. Factors affecting the formation and properties of wet compacts. *Powder Technol.* 65, 283–292.

Watanabe, Y., Kubo, K., Sato, S., 1999. Application of amphoteric polyelectrolytes for sludge dewatering. *Langmuir* 15, 4157–4164.

Wu, C.C., Wu, J.J., Huang, R.Y., 2003. Floc strength and dewatering efficiency of alum sludge. *Adv. Environ. Res.* 7, 617–621.

Zhao, J., Wang, C.H., Lee, D.J., Tien, C., 2003a. Plastic deformation in cake consolidation. *J. Colloid Interface Sci.* 261, 133–145.

Zhao, J., Wang, C.H., Lee, D.J., Tien, C., 2003b. Cake consolidation in a compression permeability cell: effect of side-wall friction. *J. Colloid Interface Sci.* 262, 60–72.